ЖЭТФ, 2008, том 134, вып. 2 (8), стр. 221–230

PHOTOIONIZATION OF THE OUTER ELECTRONS IN NOBLE GAS ENDOHEDRAL ATOMS

M. Ya. Amusia [a,b*], ***A. S. Baltenkov*** [c], ***L. V. Chernysheva*** [b]

[a] *Racah Institute of Physics, the Hebrew University 91904, Jerusalem, Israel*

[b] *Ioffe Physical-Technical Institute, Russian Academy of Sciences 194021, St.-Petersburg, Russia*

[c] *Arifov Institute of Electronics, Academy of Sciences of the Republic of Uzbekistan 700125, Tashkent, Uzbekistan*

Received February 18, 2008

We suggest a prominent modification of the outer shell photoionization cross section in noble gas (NG) endohedral atoms $NG@C_n$ under the action of the fullerene C_n electron shell. This shell leads to two important effects: a strong enhancement of the cross section due to the fullerene shell polarization under the action of the incoming electromagnetic wave and to prominent oscillation of this cross section due to the reflection of a photoelectron from NG by the fullerene shell. Both factors lead to the formation of powerful maxima in the outer shell ionization cross sections of $NG@C_n$, which we call the giant endohedral resonances. The oscillator strength reaches a very large value in the atomic scale, 25. We consider atoms of all noble gases except He. The polarization of the fullerene shell is expressed in terms of the total photoabsorption cross section of the fullerene. The photoelectron reflection is taken into account in the framework of the so-called bubble potential, which is a spherical δ-type potential. It is assumed in the derivations that NG is centrally located in the fullerene. It is also assumed, in accordance with the existing experimental data, that the fullerene radius R_C is much larger than the atomic radius r_A and the thickness Δ_C of the fullerene shell. As was demonstrated recently, these assumptions allow representing the $NG@C_n$ photoionization cross section as a product of the NG cross section and two well-defined calculated factors.

PACS: 31.15.V-, 32.80.-t, 32.80.Fb

1. INTRODUCTION

We consider the photoionization of outer shells of noble gas (NG) endohedral atoms, formed by a fullerene C_n inside which a noble-gas atom is located, $NG@C_n$. We present data on all noble gases except He. In concrete calculations, we consider C_{60} as a fullerene [1].

Presently, much attention is concentrated on photoionization of endohedral atoms. It was demonstrated in a number of papers [2–10] that the C_{60} shell adds a prominent resonance structure in the photoionization cross section of an atom A "caged" in the fullerene shell forming an endohedral atom. Although the experimental investigation of $A@C_{60}$ photoionization seems to be currently very difficult, it will be inevitably intensively studied in the nearest future[1)]. This justifies the current efforts of theorists to predict rather nontrivial effects awaiting verification.

The role of C_{60} in $NG@C_{60}$ photoionization is manifold. The electron shell of C_{60} acts as a spherical potential resonator that reflects the photoelectron wave coming from an NG atom. This leads to the interference of the outgoing and incoming (reflected) waves and to confinement resonances or simply to oscillations in the frequency dependence of the photoionization cross sections [6]. The interference of the photo-

*E-mail: amusia@vms.huji.ac.il

[1)] As first examples of such a research, we mention the data on measurements of the photoionization cross section of $Ce@C_{82}$ and some other endohedrals with a $4d$–$4f$ transition [10] and $Ce@C_{82}^+$ [11].

electron spherical waves inside the C_{60} resonator affects significantly not only the total cross section but also the angular distribution of photoelectrons. This phenomenon was analysed in Ref. [7], where it was shown that the effects of confinement resonances are also found in the frequency dependences of the dipole and nondipole parameters of the photoelectron angular distribution. The results of these studies give evidence that the reflection and refraction of the photoelectron waves by the potential C_{60} resonator are significant up to the photoelectron energy 60–80 eV.

The C_{60} shell acts as a dynamic screen that in principle, depending on the photon frequency, can suppress or enhance the incident electromagnetic radiation acting on the doped atom A [12–14]. This effect is due to polarization of the collectivized electrons of the fullerene shell by the incoming photon beam. Plasma excitations of these electrons generate an alternating dipole moment. This dipole moment causes the ionization of the electronic shells of the endohedral atom. The screening effects of the C_{60} shell are particularly strong for the incident radiation frequency ω close to the C_{60} giant resonance, i. e., 20–22 eV, but are large enough in a much broader region, from the ionization threshold up to 60–80 eV [2)].

We show in this paper that the dynamic polarization of C_{60} in fact increases the outer shell photoionization cross section at any ω, contrary to the statements in Ref. [12]. The maximal enhancement is in the region of the C_{60} dipole polarizability maximum.

Thus, the resonator and dynamic screen effects of the fullerene C_{60} shell manifest themselves as a considerable enhancement of the cross section modulated by an oscillating structure that appears due to reflection and refraction of the photoelectron wave by the fullerene shell.

We have previously studied the effect of C_{60} on the most important atomic resonances, the giant [15, 16] and interference [13], both in Xe, and found essential modifications of them. But we did not consider the modification of the outer shell, although by far the greatest part of the absolute cross section comes from the near-threshold region of the outer subshell. This drawback of all the considerations is corrected in this paper.

In the case of $Xe@C_{60}$, we demonstrated recently [17] that a powerful maximum, called the giant endohedral resonance (GER), is created in the outer shell. We show here that similar structures appear in $Ar@C_{60}$ and $Kr@C_{60}$ while the GER in $Ne@C_{60}$ is much weaker. In addition, we calculate the dipole and nondipole angular anisotropy parameters for all the atoms considered.

It would be interesting to see the alteration of the photoionization cross section if other fullerenes, like C_{70}, C_{76}, C_{82}, or C_{87}, are considered instead of C_{60}. But studying the endohedrals $NG@C_n$ with $C_n = C_{70}$, C_{76}, C_{82}, C_{87} requires knowing the shape of these objects, their photoionization cross sections, and the position of the NG atoms inside the fullerene cage. The answers to these questions are presently unavailable.

Generally speaking, there is no doubt about the existence of sufficiently pronounced oscillations due to the photoelectron reflection by any fullerene shell. But the possibility of enhancement due to the fullerene shell dynamic polarization is much more problematic.

2. MAIN FORMULAS

We use the theoretical approaches already developed in a number of previous papers [13–15]. For completeness, we recall the main points of the consideration and present the essential formulas used in the calculations.

We start with the problem of an isolated closed-shell atom. The differential-in-angle photoionization cross section by nonpolarized light of frequency ω is given by [18, 19]

$$\frac{d\sigma_{nl}(\omega)}{d\Omega} = \frac{\sigma_{nl}(\omega)}{4\pi}\left[1 - \frac{\beta_{nl}}{2}P_2(\cos\theta) + \right.$$
$$\left. + \kappa\gamma_{nl}P_1(\cos\theta) + \kappa\eta_{nl}P_3(\cos\theta)\right], \quad (1)$$

where $\kappa = \omega/c$, $P_l(\cos\theta)$ are the Legendre polynomials, θ is the angle between the photon momentum $\boldsymbol{\kappa}$ and the photoelectron velocity $\mathbf{v}$, $\beta_{nl}(\omega)$ is the dipole angular anisotropy parameter and $\gamma_{nl}(\omega)$ and $\eta_{nl}(\omega)$ are the so-called nondipole angular anisotropy parameters.

In experiment, sources of linearly polarized radiation are typically used, and therefore another form of the angular distribution is more convenient than (1) [20, 21],

$$\frac{d\sigma_{nl}(\omega)}{d\Omega} = \frac{\sigma_{nl}(\omega)}{4\pi}\left[1 + \beta_{nl}P_2(\cos\Theta) + \right.$$
$$\left. + (\delta^C_{nl} + \gamma^C_{nl}\cos^2\Theta)\sin\Theta\cos\Phi\right]. \quad (2)$$

Here, Θ is the polar angle between the vectors of photoelectron velocity $\mathbf{v}$ and photon polarization $\mathbf{e}$, and Φ is the azimuth angle determined by the projection of $\mathbf{v}$ on the plane orthogonal to $\mathbf{e}$ that includes the photon

[2)] The atomic system of units is used in this paper.

velocity vector. The nondipole parameters in (1) and (2) are connected by the simple relations [20]

$$\frac{\gamma^C_{nl}}{5} + \delta^C_{nl} = \kappa\gamma_{nl}, \quad \frac{\gamma^C_{nl}}{5} = -\kappa\eta_{nl}. \tag{3}$$

The concrete results of calculations of nondipole parameters given below are obtained using expression (2). There are two possible dipole transitions from a subshell l, $l \to l \pm 1$, and three quadrupole transitions $l \to l, l \pm 2$. The corresponding general expressions for $\beta_{nl}(\omega)$, $\gamma_{nl}(\omega)$, and $\eta_{nl}(\omega)$ are rather complex and are presented as combinations of the dipole $d_{l\pm1}$ and quadrupole $q_{l\pm2,0}$ matrix elements of photoelectron transitions and photoelectron wave phases. In the one-electron Hartree–Fock (HF) approximation, these parameters are given by [22]

$$\begin{aligned}\beta_{nl}(\omega) = {} & \frac{1}{(2l+1)\left[(l+1)\,d^2_{l+1} + l d^2_{l-1}\right]} \times \\ & \times \left[(l+1)(l+2)\,d^2_{l+1} + l(l-1)\,d^2_{l-1} - \right. \\ & \left. - 6l(l+1)\,d_{l+1}d_{l-1}\cos(\delta_{l+1} - \delta_{l-1})\right]. \end{aligned} \tag{4}$$

The parameters $\gamma_{nl}(\omega)$ and $\eta_{nl}(\omega)$ are given by the expressions [19]

$$\begin{aligned}\gamma_{nl}(\omega) = {} & \frac{3}{5\left[l d^2_{l-1} + (l+1)\,d^2_{l+1}\right]} \times \\ & \times \left\{ \frac{l+1}{2l+3}\left[3(l+2)q_{l+2}d_{l+1}\cos(\delta_{l+2} - \delta_{l+1}) - \right.\right. \\ & \left. - l q_l d_{l+1}\cos(\delta_{l+2} - \delta_{l+1})\right] - \\ & - \frac{l}{2l+1}\left[3(l-1)q_{l-2}d_{l-1}\cos(\delta_{l-2} - \delta_{l-1}) - \right. \\ & \left.\left. - (l+1)q_l d_{l-1}\cos(\delta_l - \delta_{l-1})\right]\right\}, \end{aligned} \tag{5}$$

$$\begin{aligned}\eta_{nl}(\omega) = {} & \frac{3}{5\left[l d^2_{l-1} + (l+1)\,d^2_{l+1}\right]} \times \\ & \times \left\{ \frac{(l+1)(l+2)}{(2l+1)(2l+3)} q_{l+2}\left[5l d_{l-1}\cos(\delta_{l+2} - \delta_{l-1}) - \right.\right. \\ & \left. - (l+3)\,d_{l+1}\cos(\delta_{l+2} - \delta_{l-1})\right] - \\ & - \frac{(l-1)l}{(2l+1)(2l+1)} q_{l-2}\left[5(l+1)\,d_{l+1}\cos(\delta_{l-2} - \delta_{l+1}) - \right. \\ & \left. - (l-2)\,d_{l-1}\cos(\delta_{l-2} - \delta_{l-1})\right] + \\ & + 2\frac{l(l+1)}{(2l-1)(2l+3)} q_l\left[(l+2)\,d_{l+1}\cos(\delta_l - \delta_{l+1}) - \right. \\ & \left.\left. - (l-1)\,d_{l-1}\cos(\delta_l - \delta_{l-1})\right]\right\}, \end{aligned} \tag{6}$$

where $\delta_l(\kappa)$ are the photoelectron scattering phases. The following relation gives the matrix elements $d_{l\pm1}$ in the so-called r-form:

$$d_{l\pm1} \equiv \int_0^\infty P_{nl}(r) r P_{\varepsilon l\pm1}(r)\,dr, \tag{7}$$

where $P_{nl}(r)$ and $P_{\varepsilon l\pm1}(r)$ are the radial HF one-electron wave functions of the nl discrete level and $\varepsilon l \pm 1$ level in continuous spectrum [22]. The quadrupole matrix elements are given by

$$q_{l\pm2,0} \equiv \frac{1}{2}\int_0^\infty P_{nl}(r) r^2 P_{\varepsilon l\pm2,0}(r)\,dr. \tag{8}$$

In the random-phase approximation with exchange (RPAE) [22] multielectron correlations, the following substitutions are made in the expressions for $\beta_{nl}(\omega)$, $\gamma_{nl}(\omega)$, and $\eta_{nl}(\omega)$ [19]:

$$\begin{aligned} d_{l+1}d_{l-1}\cos(\delta_{l+1} - \delta_{l-1}) \to {} & [(\operatorname{Re} D_{l+1}\operatorname{Re} D_{l-1} + \\ & + \operatorname{Im} D_{l+1}\operatorname{Im} D_{l-1})\cos(\delta_{l+1} - \delta_{l-1}) - \\ & - (\operatorname{Re} D_{l+1}\operatorname{Im} D_{l-1} - \operatorname{Im} D_{l+1}\operatorname{Re} D_{l-1}) \times \\ & \times \sin(\delta_{l+1} - \delta_{l-1})] \equiv \\ \equiv {} & \tilde{D}_{l+1}\tilde{D}_{l-1}\cos(\delta_{l+1} + \Delta_{l+1} - \delta_{l-1} - \Delta_{l-1}), \end{aligned} \tag{9}$$

$$\begin{aligned} d_{l\pm1}q_{l\pm2,0}\cos(\delta_{l\pm2,0} - \delta_{l\pm1}) \to {} & [(\operatorname{Re} D_{l\pm1}\operatorname{Re} Q_{l\pm2,0} + \\ & + \operatorname{Im} D_{l\pm1}\operatorname{Im} Q_{l\pm2,0})\cos(\delta_{l\pm2,0} - \delta_{l\pm1}) - \\ & - (\operatorname{Re} D_{l\pm1}\operatorname{Im} Q_{l\pm2,0} - \operatorname{Im} D_{l\pm1}\operatorname{Re} Q_{l\pm2,0}) \times \\ & \times \sin(\delta_{l\pm2,0} - \delta_{l\pm1})] \equiv \tilde{D}_{l\pm1}\tilde{Q}_{l\pm2,0} \times \\ & \times \cos(\delta_{l\pm2,0} + \Delta_{l\pm2,0} - \delta_{l\pm1} - \Delta_{l\pm1}). \end{aligned} \tag{10}$$

$$d^2_{l\pm1} \to \operatorname{Re} D^2_{l\pm1} + \operatorname{Im} D^2_{l\pm1} \equiv \tilde{D}^2_{l\pm1}.$$

For matrix elements with multielectron (respectively, dipole and quadrupole) correlations taken into account, we here use the notation

$$\begin{aligned} D_{l\pm1}(\omega) &\equiv \tilde{D}_{l\pm1}(\omega)\exp\left[i\Delta_{l\pm1}(\varepsilon)\right], \\ Q_{l\pm2,0}(\omega) &\equiv \tilde{Q}_{l\pm2,0}(\omega)\exp\left[i\Delta_{l\pm2,0}(\varepsilon)\right], \end{aligned} \tag{11}$$

where $\tilde{D}_{l\pm1}(\omega)$, $\tilde{Q}_{l\pm2,0}(\omega)$, $\Delta_{l\pm1}$, and $\Delta_{l\pm2,0}$ are absolute values of the amplitudes for the respective transitions and phases for photoelectrons with angular momenta $l \pm 1$ and $l \pm 2, 0$.

The RPAE equation for the dipole matrix elements is [22]

$$\begin{aligned} \langle\nu_2|D(\omega)|\nu_1\rangle = {} & \langle\nu_2|d|\nu_1\rangle + \\ & + \sum_{\nu_3,\nu_4} \frac{\langle\nu_3|D(\omega)|\nu_4\rangle(n_{\nu_4} - n_{\nu_3})\langle\nu_4\nu_2|U|\nu_3\nu_1\rangle}{\varepsilon_{\nu_4} - \varepsilon_{\nu_3} + \omega + i\eta(1 - 2n_{\nu_3})}, \end{aligned} \tag{12}$$

where

$$\langle\nu_1\nu_2|U|\nu_1'\nu_2'\rangle \equiv \langle\nu_1\nu_2|V|\nu_1'\nu_2'\rangle - \langle\nu_1\nu_2|V|\nu_2'\nu_1'\rangle, \quad (13)$$

$V \equiv 1/|\mathbf{r}-\mathbf{r}'|$, ν_i is the total set of quantum numbers that characterize a HF one-electron state on discrete (continuum) levels, ε_{ν_i} are the HF energies, and $\eta \to +0$. This set includes the principal quantum number (energy), the angular momentum, its projection, and the projection of the electron spin. The function n_{ν_i} (the so-called step function) is equal to unity for occupied and zero for vacant states.

The dipole matrix elements $D_{l\pm1}$ are obtained by solving the radial part of RPAE equation (12). The quadrupole matrix elements $Q_{l\pm2,0}$ are obtained by solving the radial part of a RPAE equation similar to (12),

$$\langle\nu_2|Q(\omega)|\nu_1\rangle = \langle\nu_2|\hat{q}|\nu_1\rangle + \\ + \sum_{\nu_3,\nu_4} \frac{\langle\nu_3|Q(\omega)|\nu_4\rangle(n_{\nu_4}-n_{\nu_3})\langle\nu_4\nu_2|U|\nu_3\nu_1\rangle}{\varepsilon_{\nu_4}-\varepsilon_{\nu_3}+\omega+i\eta(1-2n_{\nu_3})}, \quad (14)$$

where $\hat{q} = r^2 P_2(\cos\theta)$ in the r-form.

Equations (12) and (14) are solved numerically using the procedure discussed at length in Ref. [23].

3. EFFECT OF THE C_{60} FULLERENE SHELL

We start with the confinement effects. Near the photoionization threshold, these effects can be described in the framework of the "orange" skin potential model. According to this model, for small photoelectron energies, the real static and not perfectly spherical potential of C_{60} can be represented by the zero-thickness bubble pseudopotential (see Refs. [24, 25] and the references therein):

$$V(r) = -V_0\delta(r-R). \quad (15)$$

The parameter V_0 is determined by the requirement that the binding energy of the extra electron in the negative C_{60}^- ion is equal to its observable value. Adding potential (15) to the atomic HF potential leads to a factor $F_l(k)$ in the photoionization amplitudes, which depends only on the photoelectron momentum k and the orbital quantum number l [24, 25]:

$$F_l(k) = \left[1 - \frac{v_{kl}(R)}{u_{kl}(R)}\operatorname{tg}\check{\Delta}_l(k)\right]\cos\check{\Delta}_l(k), \quad (16)$$

where $\check{\Delta}_l(k)$ are the additional phase shifts due to the fullerene shell potential (15). They are expressed as

$$\operatorname{tg}\check{\Delta}_l(k) = \frac{u_{kl}^2(R)}{u_{kl}(R)v_{kl}(R) + k/2V_0}. \quad (17)$$

In these formulas, $u_{kl}(r)$ and $v_{kl}(r)$ are the regular and irregular solutions of the atomic HF equations for a photoelectron with the momentum $k = \sqrt{2\varepsilon}$, where ε is the photoelectron energy related with the photon energy ω by the relation $\varepsilon = \omega - I_A$ with I_A being the atom A ionization potential.

Using Eq. (16), we can express the $D^{AC(r)}$ and $Q^{AC(r)}$ amplitudes for an endohedral atom A@C_{60}, with photoelectron reflection and refraction by the C_{60} static potential (15) taken into account, in terms of the respective values corresponding to $nl \to \varepsilon l'$ transitions for an isolated atom:

$$D^{AC(r)}_{nl,kl'}(\omega) = F_{l'}(k)D_{nl,kl'}(\omega), \\ Q^{AC(r)}_{nl,kl''}(\omega) = F_{l''}(k)Q_{nl,kl''}(\omega). \quad (18)$$

For the cross sections, we have

$$\sigma^{AC(r)}_{nl,kl'}(\omega) = F^2_{l'}(k)\sigma^{A}_{nl,kl'}(\omega), \quad (19)$$

where $\sigma^{A}_{nl,kl'}(\omega)$ is the contribution of the $nl \to \varepsilon l'$ transition to the photoionization cross section of the atomic subshell nl, $\sigma^{A}_{nl}(\omega)$.

We now discuss the role of polarization of the C_{60} shell under the action of a photon beam [13]. The effect of the fullerene electron shell polarization on the atomic photoionization amplitude can be taken into account in the RPAE using Eq. (12). This approximation is good for isolated atoms [22], and it is reasonable to assume that it is also good for endohedral atoms.

Symbolically, by applying Eq. (12) to the whole NG@C_n system, we can represent the total amplitude $\hat{D}_A$ of the electron photoionization of a caged atom as a sum of two terms:

$$\hat{D}_A = \hat{d}_A + \hat{D}_C\hat{\chi}U_{CA}, \quad (20)$$

where $\hat{D}_C$ is the ionization amplitude of any electrons other than the electrons of the atom A (A-electrons),

$$\hat{\chi} = \frac{1}{\omega - \hat{H}_{ev}} - \frac{1}{\omega + \hat{H}_{ev}}$$

is the propagator of other electron excitations, i.e., the electron (e)–vacancy (v) pair creation, and $\hat{H}_{ev}$ is the pair HF Hamiltonian. The interaction terms in Eq. (13) can be written as

$$U_{CA} \equiv V_{CAdir} - V_{CAexc},$$

with V_{CAdir} and V_{CAexc} being the operators of the direct and exchange pure Coulomb interaction between C- and A-electrons.

Formula (20) is simplified considerably if the A-electrons are at much smaller distances from the

center of the system than the C-electrons. Then the Coulomb interaction is considerably simplified, becoming

$$U_{\mathrm{CA}} \approx \mathbf{r}_{\mathrm{C}} \cdot \mathbf{r}_{\mathrm{A}}/r_{\mathrm{C}}^3, \quad r_{\mathrm{C}} \gg r_{\mathrm{A}}, \tag{21}$$

where $\mathbf{r}_{\mathrm{A}}$ and $\mathbf{r}_{\mathrm{C}}$ are the A- and C-electron shell radii.

In the language of many-body diagrams [22], expression (20) can be represented as

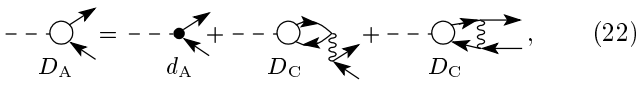

(22)

where the dashed line, the line with an arrow pointing right (left), and the wavy line respectively represent the incoming photon, the electron, the vacancy, and the direct (exchange) Coulomb A–C-electrons interaction.

Equations (20) and (22) can be easily generalized in the spirit of the Landau Fermi-liquid theory by incorporating all nonsimple electron–vacancy excitations (for example, two electrons–two vacancies excitations of the A-shell into d_{A}) [22].

The effect of the C-shell is represented especially simple for an inner shell located well inside the intermediate and outer atomic subshells. Then rightfully neglecting the exchange A–C-interaction and representing U_{AC} as in Eq. (21), we reduce Eq. (20) to an algebraic equation (instead of an operator equation), where $\hat{D}_{\mathrm{C}}\hat{\chi}U_{\mathrm{CA}}$ is substituted by the expression

$$\frac{2}{\overline{r}_{\mathrm{C}}^3} \sum_{evexc,\mathrm{C}} \frac{\omega_{ev} D_{ev}(\omega)}{\omega^2 - \omega_{ev}^2}\, d_{ev} \equiv -\frac{\alpha_{\mathrm{C}}(\omega)}{\overline{r}_{\mathrm{C}}^3}. \tag{23}$$

Here, the summation over "$evexc$,C" ranges all electron–vacancy excitations of the considered shell. Some more complex excitations are included into the amplitude $D_{ev}(\omega)$; $\overline{r}_{\mathrm{C}}$ is the mean radius of the C-shell. In Eq. (23), we use an alternative definition of the dipole polarizability $\alpha_{\mathrm{C}}(\omega)$ of the C-shell, or in our case, the fullerene C_{60}. Usually, $\alpha_{\mathrm{C}}(\omega)$ is defined as

$$\alpha_{\mathrm{C}}(\omega) \equiv -2 \sum_{evexc,\mathrm{C}} \frac{\omega_{ev} |D_{ev}(\omega_{ev})|^2}{\omega^2 - \omega_{ev}^2}, \tag{24}$$

but it can be easily demonstrated that this definition and that in Eq. (23) are identical (see, e. g., Ref. [22]).

Instead of Eq. (20), we therefore have the formula [22]

$$D_{\mathrm{A}}(\omega) \approx d_{\mathrm{A}} \left(1 - \frac{\alpha_{\mathrm{C}}(\omega)}{\overline{r}_{\mathrm{C}}^3}\right). \tag{25}$$

In accordance with the observed features of C_{60}, we assume, that the electrons are located within a layer whose thickness Δ_{C} is much smaller than R_{C}. We can therefore replace $\overline{r}_{\mathrm{C}}$ with the fullerene radius R_{C}. Hence, the amplitude $D^{\mathrm{AC}}_{nl,\varepsilon l'}(\omega)$ of the endohedral atom photoionization due to an $nl \to \varepsilon l'$ transition with all the essential atomic correlations taken into account can be written as [13]

$$D^{\mathrm{AC}}_{nl,\varepsilon l'}(\omega) \approx F_{l'}(k) \left[1 - \frac{\alpha^d_{\mathrm{C}}(\omega)}{R_{\mathrm{C}}^3}\right] D^{\mathrm{A}}_{nl,\varepsilon l'}(\omega) \equiv \equiv F_{l'}(k) G^d(\omega) D^{\mathrm{A}}_{nl,\varepsilon l'}(\omega), \tag{26}$$

where $\alpha^d_{\mathrm{C}}(\omega)$ is the dipole dynamic polarizability of C_{60} and $D^{\mathrm{A}}_{nl,\varepsilon l'}(\omega)$ accounts for all the electron correlations in the caged atom. For the quadrupole amplitude, a similar expression can be obtained starting from Eq. (14):

$$Q^{\mathrm{AC}}_{nl,\varepsilon l'}(\omega) \approx F_{l'}(k) \left[1 - \frac{1}{2}\,\frac{\alpha^q_{\mathrm{C}}(\omega)}{R_{\mathrm{C}}^5}\right] Q^{\mathrm{A}}_{nl,\varepsilon l'}(\omega) \equiv \equiv F_{l'}(k) G^q(\omega) Q^{\mathrm{A}}_{nl,\varepsilon l'}(\omega), \tag{27}$$

where $\alpha^q_{\mathrm{C}}(\omega)$ is the quadrupole dynamic polarizability of C_{60}. The $G^{d,q}(\omega)$ factors are complex numbers that we represent as

$$G^{d,q}(\omega) = \tilde{G}^{d,q}(\omega) \exp\left[i\eta^{d,q}(\omega)\right], \tag{28}$$

where $\tilde{G}^{d,q}(\omega)$ are corresponding absolute values.

Using the relation

$$\sigma^d_{\mathrm{C}}(\omega) \sim \operatorname{Im} \alpha^d_{\mathrm{C}}(\omega) = c\sigma^d_{\mathrm{C}}(\omega)/4\pi\omega$$

between the imaginary part of the polarizability and the dipole photoabsorption cross section, we can derive the polarizability of the C_{60} shell. Although experiments [27, 28] do not provide absolute values of $\sigma^d_{\mathrm{C}}(\omega)$, they can be reliably estimated using different normalization procedures based on sum rule

$$\frac{c}{2\pi^2} \int\limits_{I_{\mathrm{C}}}^{\infty} \sigma^d_{\mathrm{C}}(\omega)\, d\omega = N,$$

where N is the number of collectivized electrons and I_{C} is the C_{60} ionization potential. The real part of polarizability is related with the imaginary one (and with the photoabsorption cross section) by the dispersion relation

$$\operatorname{Re} \alpha^d_{\mathrm{C}}(\omega) = \frac{c}{2\pi^2} \int\limits_{I_{\mathrm{C}}}^{\infty} \frac{\sigma^d_{\mathrm{C}}(\omega')\, d\omega'}{\omega'^2 - \omega^2}. \tag{29}$$

This approach was used for polarizability of C_{60} in Ref. [14], where it was assumed that $N = 240$, which

corresponds to four collectivized electrons per each C atom in C_{60}. Using the photoabsorption data that are considered most reliable in Ref. [27], we obtain $N_{eff} \approx 250$, which is sufficiently close to the value assumed in Ref. [14].

The equality $\mathrm{Im}\,\alpha^q_{\mathrm{C}}(\omega) = c\sigma^q_{\mathrm{C}}(\omega)/4\pi\omega$ and a quadrupole dispersion relation similar to Eq. (29) hold. But the quadrupole photoabsorption cross section is so small that it cannot be derived experimentally.

We note that because the strong inequality $R_{\mathrm{C}} \gg r_{\mathrm{A}}$ (r_{A} is the atomic radius) is assumed, we have derived formulas (20) and (21) that are more accurate than those obtained from the RPAE for the whole $\mathrm{A@C}_n$ system. This is important because the one electron–one vacancy channel, which is the only one taken into account in RPAE, is not always dominant in the photoabsorption cross section of the fullerene and hence in its polarizability.

Using the amplitude in (26), we obtain the cross section

$$\sigma^{\mathrm{AC}}_{nl,\varepsilon l'}(\omega) = F^2_{l'}(\omega)\left|1 - \frac{\alpha^d_{\mathrm{C}}(\omega)}{R^3_{\mathrm{C}}}\right|^2 \sigma^{\mathrm{A}}_{nl,\varepsilon l'}(\omega) \equiv \equiv F^2_{l'}(\omega) S(\omega)\sigma^{\mathrm{A}}_{nl,\varepsilon l'}(\omega), \quad (30)$$

where $S(\omega) = [\tilde{G}^d(\omega)]^2$ can be called the radiation enhancement parameter.

With these amplitudes, using expressions (4)–(6) and performing substitution (9), (10), we obtain the cross sections for $\mathrm{NG@C}_{60}$ and angular anisotropy parameters. In calculating the anisotropy parameters, we first replace the cosines of atomic phase differences in Eqs. (4)–(6), $\cos(\delta_l - \delta_{l'})$ with $\cos(\delta_l + \Delta_l - \delta_{l'} - \Delta_{l'})$. As a result, using Eq. (9), we express the dipole angular anisotropy parameter (4) as

$$\beta_{nl}(\omega) = \frac{1}{2l+1}\left[(l+1)F^2_{l+1}\tilde{D}^2_{l+1} + lF^2_{l-1}\tilde{D}^2_{l-1}\right]^{-1} \times \times \left[(l+1)(l+2)F^2_{l+1}\tilde{D}^2_{l+1} + \right. + l(l-1)F^2_{l-1}\tilde{D}^2_{l-1} - 6l(l+1)F_{l+1}F_{l-1}\tilde{D}_{l+1}\tilde{D}_{l-1} \times \left. \times \cos\left(\tilde{\delta}_{l+1} - \tilde{\delta}_{l-1}\right)\right], \quad (31)$$

where $\tilde{\delta}_{l'} = \delta_{l'} + \Delta_{l'}$ (see Eq. (11)). Naturally, the dipole parameter $\beta_{nl}(\omega)$ is not affected by $G^d(\omega)$ factors, which alter the numerator and the denominator in Eq. (31) similarly.

The situation for nondipole parameters is different, because $G^d(\omega) \neq G^q(\omega)$. From Eqs. (5) and (6), using substitution (9), (10), we arrive at the following expressions for the nondipole angular anisotropy parameters:

$$\gamma_{nl}(\omega) = \frac{3\tilde{G}^q(\omega)}{5\tilde{G}^d(\omega)\left[(l+1)F^2_{l+1}\tilde{D}^2_{l+1} + lF^2_{l-1}\tilde{D}^2_{l-1}\right]} \times \times \left\{\frac{(l+1)F_{l+1}}{2l+3}\left[3(l+2)F_{l+2}\tilde{Q}_{l+2}\tilde{D}_{l+1} \times \right.\right. \times \cos\left(\tilde{\tilde{\delta}}_{l+2} - \tilde{\tilde{\delta}}_{l+1}\right) - lF_l\tilde{Q}_l\tilde{D}_{l+1}\cos\left(\tilde{\tilde{\delta}}_{l+2} - \tilde{\tilde{\delta}}_{l+1}\right)\Big] - -\frac{lF_{l-1}}{2l+1}\Big[3(l-1)F_{l-2}\tilde{Q}_{l-2}\tilde{D}_{l-1}\cos\left(\tilde{\tilde{\delta}}_{l-2} - \tilde{\tilde{\delta}}_{l-1}\right) - \left.\left. - (l+1)F_l\tilde{Q}_l\tilde{D}_{l-1}\cos\left(\tilde{\tilde{\delta}}_l - \tilde{\tilde{\delta}}_{l-1}\right)\right]\right\}, \quad (32)$$

$$\eta_{nl}(\omega) = \frac{3\tilde{G}^q(\omega)}{5\tilde{G}^d(\omega)\left[(l+1)F^2_{l+1}\tilde{D}^2_{l+1} + lF^2_{l-1}\tilde{D}^2_{l-1}\right]} \times \times \left\{\frac{(l+1)(l+2)}{(2l+1)(2l+3)}F_{l+2}\tilde{Q}_{l+2} \times \right. \times \Big[5lF_{l-1}\tilde{D}_{l-1}d_{l-1}\cos\left(\tilde{\tilde{\delta}}_{l+2} - \tilde{\tilde{\delta}}_{l-1}\right) - - (l+3)F_{l+1}\tilde{D}_{l+1}\cos\left(\tilde{\tilde{\delta}}_{l+2} - \tilde{\tilde{\delta}}_{l-1}\right)\Big] - - \frac{(l-1)l}{(2l+1)(2l+1)}F_{l-2}\tilde{Q}_{l-2} \times \times \Big[5(l+1)F_{l+1}\tilde{D}_{l+1}\cos\left(\tilde{\tilde{\delta}}_{l-2} - \tilde{\tilde{\delta}}_{l+1}\right) - - (l-2)\tilde{F}_{l-1}\tilde{D}_{l-1}\cos\left(\tilde{\tilde{\delta}}_{l-2} - \tilde{\tilde{\delta}}_{l-1}\right)\Big] + + 2\frac{l(l+1)F_l\tilde{Q}_l}{(2l-1)(2l+3)} \times \times \Big[(l+2)F_{l+1}\tilde{D}_{l+1}\tilde{D}_{l+1}\cos\left(\tilde{\tilde{\delta}}_l - \tilde{\tilde{\delta}}_{l+1}\right) - \left.\left. - (l-1)F_{l-1}\tilde{D}_{l-1}\tilde{D}_{l-1}\cos\left(\tilde{\tilde{\delta}}_l - \tilde{\tilde{\delta}}_{l-1}\right)\Big]\right\}, \quad (33)$$

where $\tilde{\tilde{\delta}}_{l\pm2,0} = \tilde{\delta}_{l\pm2,0} + \eta^q$ and $\tilde{\tilde{\delta}}_{l\pm1} = \tilde{\delta}_{l\pm1} + \eta^d$ (see (28)).

4. SOME DETAILS OF CALCULATIONS AND THEIR RESULTS

Naturally, the C_{60} parameters in the present calculations were chosen the same as in the previous papers, e. g., in Ref. [23]: $R_{\mathrm{C}} = 6.639$ and $V_0 = 0.443$. Having in mind the size of the fullerene radius and estimating the thickness of its shell as $\Delta \approx 2$, we can conclude that our approach works well up to the photoelectron energy 2–3 at. un.

Preliminary investigations have demonstrated that $G^q_{\mathrm{C}}(\omega)$ is close to unity. This means that the role of

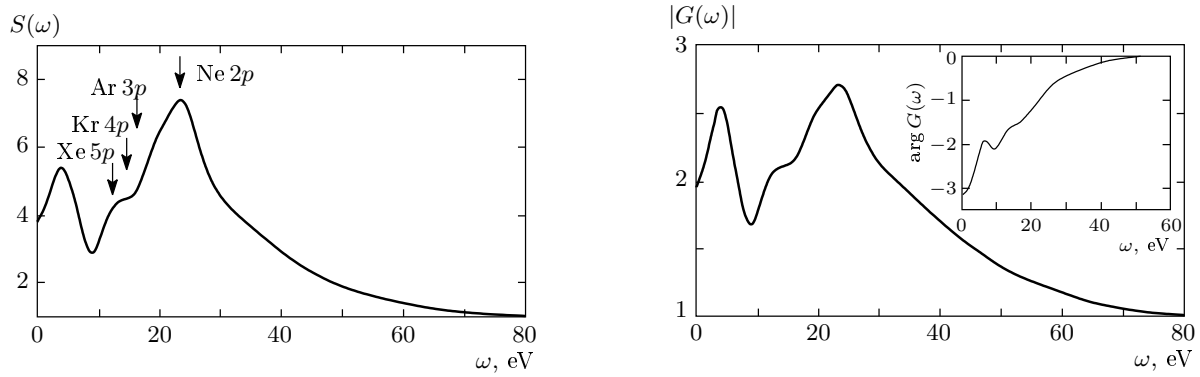

Fig. 1. Radiation enhancement parameter $S(\omega)$, the absolute value of its amplitude $\tilde{G}^d(\omega) \equiv |G(\omega)|$, and the phase $\eta^d \equiv \arg G(\omega)$. Arrows denote the threshold positions of the corresponding outer np-subshells

quadrupole polarization can be neglected. This is why we assume that $G^q_{\rm C}(\omega) = 1$ and $\eta^q = 0$ in the results presented below.

In Fig. 1, we present the radiation enhancement parameter $S(\omega)$, the absolute value of its amplitude $\tilde{G}^d(\omega) \equiv |G(\omega)|$, and the phase $\eta^d \equiv \arg G(\omega)$. It is seen that the curves are rather complex and can considerably modify the outer subshell photoionization cross section and nondipole angular anisotropy parameters.

In Ref. [17], we presented the cross section and the dipole angular anisotropy parameter for $5p$-electrons in Xe@C_{60}. Here, in Figs. 2–5, we in addition have data for the outer shell photoionization cross section and the dipole and nondipole angular anisotropy parameters of outer p-electrons in NG@C_{60}, where NG = Ne, Ar, Kr, Xe.

Figure 2 depicts the photoionization cross section and the dipole and nondipole angular anisotropy parameters for $2p$-electrons of Ne@C_{60}. Similarly, the same characteristics are presented in Figs. 3–5 for Ar@C_{60}, Kr@C_{60}, and Xe@C_{60}.

In all the cases considered, we see a prominent influence of the fullerene shell on the photoionization of the caged atom (Ne, Ar, Kr, and Xe). Most impressive is the increase in the photoionization cross section, which reaches a factor of fifteen to twenty. The absolute value of the cross section reaches tremendous values in the atomic scale, up to 1000 Mb.

The maxima in the upper curves in Figs. 2–5 may be reasonably called the giant endohedral resonance (GER). Without a doubt, a similar effect occurs in outer shells of other endohedral atoms and in atoms caged by other fullerenes than C_{60}. It is quite probable that such resonances can be detected in experimental studies of photoionization of endohedral atoms, using the photoelectron spectroscopy methods.

The GER in photoionization of Ar@C_{60}, Kr@C_{60}, and Xe@C_{60} impressively exceeds the atomic giant resonance in the photoionization cross section of Xe $4d$-electrons. The monotonically decreasing curves in isolated atoms are transformed into curves with two maxima (one large and the other much smaller) with a remarkably large total oscillator strength of about 25, i. e., 2.5 times larger than that of the $4d$-atomic giant resonance in isolated Xe. Due to this increase in the caged atom photoionization cross section, the total oscillator strength sum in the ω range, e. g., $I < \omega < I + 1$ Ry, increases dramatically.

A natural question is: what is the origin of this increase? The answer is as follows. This increase comes from the fullerene shell, and is not caused by a redistribution of the caged atom oscillator strength. This latter is evident because this atom just does not have enough electrons for this. We note that the total sum rule for an endohedral atom is equal to $N_{C_n} + N_A$, where N_{C_n} and N_A are the total numbers of electrons in the fullerene and the atom. As regards the sum of oscillator strengths of the caged atom, it increases, roughly speaking, by the area between the solid and dash-and-dot curves in Figs. 2–5.

The effect of the oscillator strength due to electron correlations moving from one part of the photon spectrum to another also occurs in isolated atoms. Indeed, it is well known that the dipole sum rule is valid only for the total atom. Approximately, however, it also holds for multielectron subshells [22]. But it does not hold for few-electron shells; for endohedrals, their role is played by outer shells of atoms caged inside C_{60}. As was discussed in Ref. [13], the behavior of the $5s$-subshell in

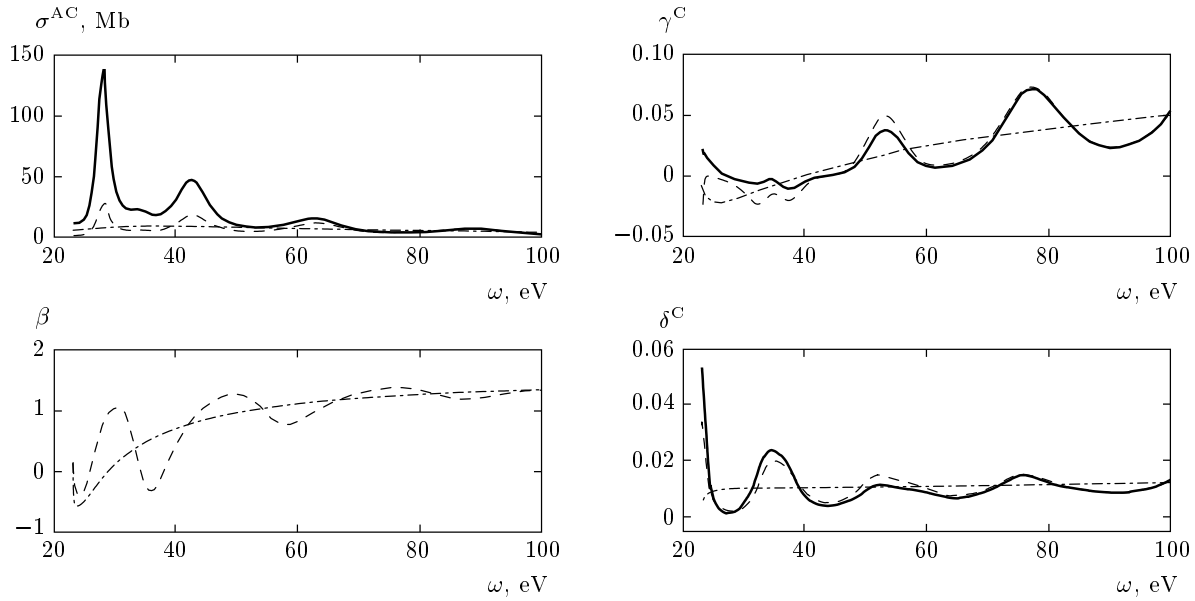

Fig. 2. Photoionization cross sections and the angular anisotropy dipole β and nondipole γ^C and δ^C parameters for $2p$-electrons of $Ne@C_{60}$: the dash-and-dot, dashed, and solid lines are for free Ne atom, $Ne@C_{60}$, and $Ne@C_{60}$ with account of C_{60} plasma excitations, respectively

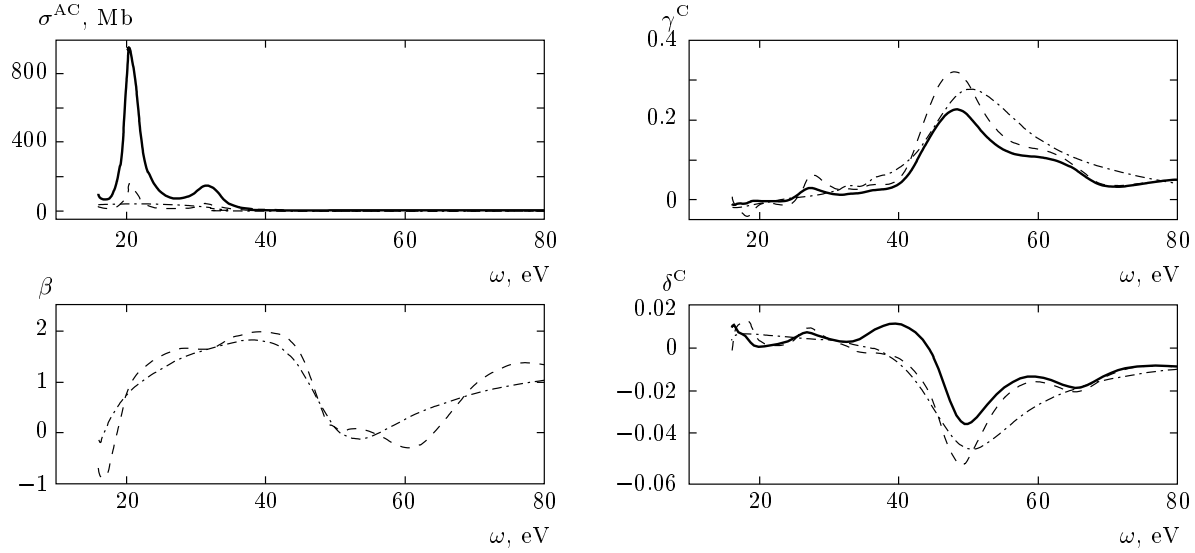

Fig. 3. The same as in Fig. 2 for $3p$-electrons of $Ar@C_{60}$

Xe is similar to that of caged-atom electrons in $A@C_{60}$. For example, if we compare the total oscillator strength of the $5s$-subshell without and with taking the action of $4d$- and $5p$-electrons on $5s$ into account, they differ by a factor of two.

In calculating the sum rules, we consider only 240 collectivized electrons of the C_{60}, neglecting the contribution of 120 electrons tightly bound to the C nuclei. This is possible because the ionization threshold for these electrons is 284.2 eV, which is much larger than the outer subshell ionization potential and total photon energies in the region of interest, $\omega < 30$–50 eV. The interaction between such remote subshells is inessential, and they cannot affect each other total oscillator strengths.

The effect of photoelectron reflection on the dipole

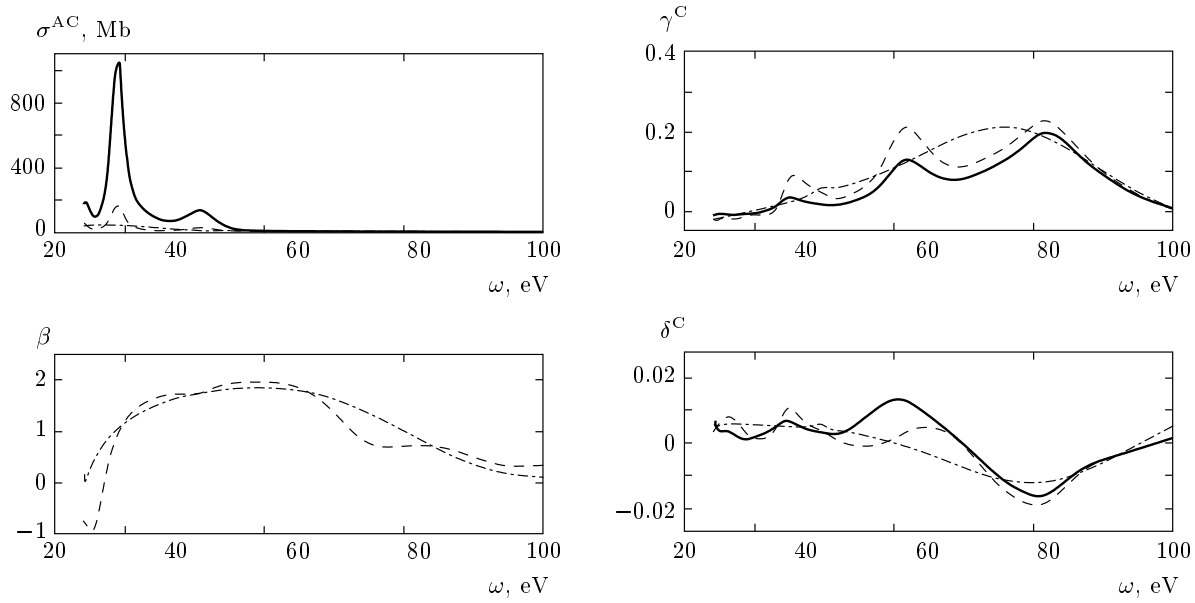

Fig. 4. The same as in Fig. 2 for $4p$-electrons of $Kr@C_{60}$

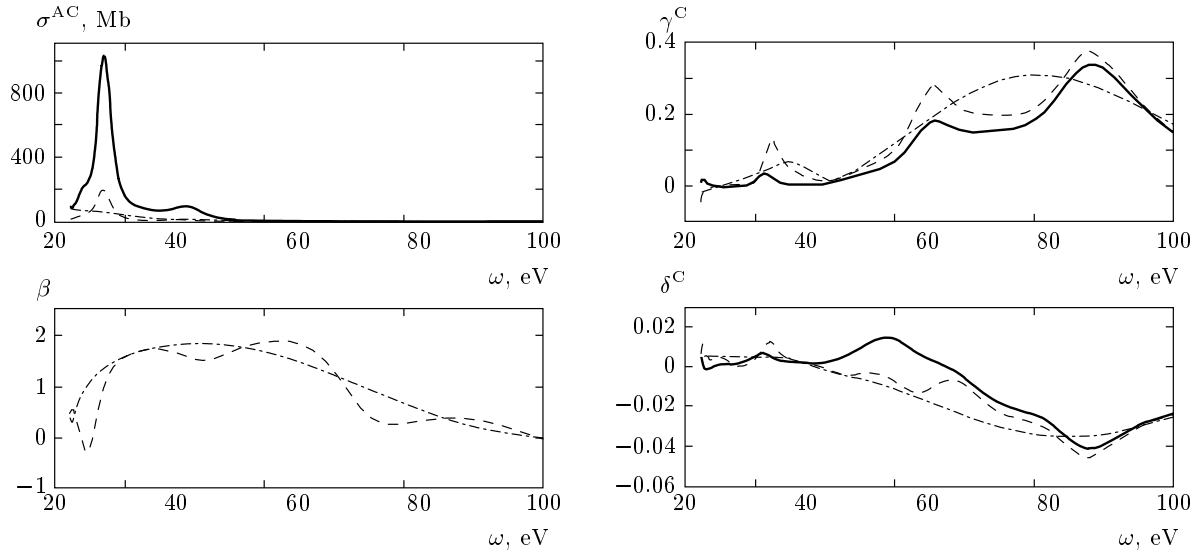

Fig. 5. The same as in Fig. 2 for $5p$-electrons of $Xe@C_{60}$

angular anisotropy parameter β is illustrated by the curves in Figs. 2–5. It can be seen that fullerene shells add oscillations that are particularly strong in Ne and Xe. Nondipole parameters γ and η are shown in Figs. 2–5 for Ne, Ar, Kr, and Xe. Here, the reflection of photoelectrons by the fullerene shell leads to oscillations, while the polarization of the shell results in a significant decrease in γ^C. This parameter is weakly dependent on the phase η. As regards δ^C, it is much smaller than γ^C but much more sensitive to η. As a result, δ^C varies in a more sophisticated way than γ^C.

5. GENERAL DISCUSSION

As a fullerene, we considered only C_{60}. As was mentioned in Introduction, it would be interesting to see the alteration of the photoionization cross section if other fullerenes, like C_{70}, C_{76}, C_{82}, or C_{87}, are considered instead of C_{60}. We do not know the shape and

photoionization cross sections of C_{70}, C_{76}, C_{82}, or C_{87} and the position of the NG atoms inside the fullerenes. However, to have the feeling of the fullerene shell effect on the photoionization of NG, we can use the results for C_{60} by scaling them to another radius, the number of collectivized electrons, etc. Because the effects of radiative enhancement and oscillations due to reflection are sensitive to the radius, the fullerene potential, and the number of electrons in it, we can expect quite different behavior for other fullerenes than C_{60}.

It is essential to have in mind that the "caged" atoms can be ionized. The electrons go to the fullerene shell, which becomes not a neutral but a negatively charged surface. This requires a modification in taking the reflection of photoelectrons by the fullerene shell into account. The shell cannot be considered neutral and described by a zero-thickness potential; instead, it is to be combined with a Coulomb long-range potential. Such a modification, although straightforward, considerably complicates the calculation procedure that leads to a rather simple $F_l(k)$ factor in this paper.

One of the authors (M. Ya. A.) is grateful for a financial support to the Israeli Science Foundation (Grant 174/03) and the Hebrew University Intramural Funds. Another author (A. S. B.) expresses his gratitude to the Hebrew University for hospitality and to the Uzbekistan National Foundation (Grant Ф-2-1-12) for the financial support.

REFERENCES

1. M. Ya. Amusia, A. S. Baltenkov, and L. V. Chernysheva, arXiv:0710.3910.
2. M. J. Pushka and R. M. Niemenen, Phys. Rev. B **47**, 1181 (1993).
3. G. Wendin and B. Wastberg, Phys. Rev. B **48**, 14764 (1993).
4. L. S. Wang, J. M. Alford, Y. Chai et al., Z. Phys. D **26**, S297 (1993).
5. P. Decleva, G. De Alti, and M. Stener, J. Phys. B **32**, 4523 (1999).
6. J.-P. Connerade, V. K. Dolmatov, and S. T. Manson, J. Phys. B **33**, 2279 (2000).
7. J. P. Connerade, V. K. Dolmatov, and S. T. Manson, J. Phys. B **33**, L275 (2000).
8. H. Shinohara, Rep. Progr. Phys. **63**, 843 (2000).
9. M. Stener, G. Fronzoni, D. Toffoli et al., J. Phys. B **35**, 1421 (2002).
10. K. Mitsuke, T. Mori, J. Kou et al., J. Chem. Phys. **122**, 064304 (2005).
11. A. Muller, S. Schippers, R. A. Phaneuf et al., J. Phys.: Conf. Series **88**, 012038 (2007).
12. J.-P. Connerade and A. V. Solov'yov, J. Phys. B **38**, 807 (2005).
13. M. Ya. Amusia and A. S. Baltenkov, Phys. Rev. A **73**, 062723 (2006).
14. M. Ya. Amusia and A. S. Baltenkov, Phys. Lett. A **360**, 294 (2006).
15. M. Ya. Amusia, A. S. Baltenkov, L. V. Chernysheva et al., Zh. Exp. Teor. Fiz. **129**, 63 (2006).
16. M. Ya. Amusia, A. S. Baltenkov, L. V. Chernysheva et al., J. Phys. B **38**, L169 (2005).
17. M. Ya. Amusia, A. S. Baltenkov, and L. V. Chernysheva, Pis'ma v Zh. Eksp. Teor. Fiz. **87**, 230 (2008).
18. M. Ya. Amusia, P. U. Arifov, A. S. Baltenkov et al., Phys. Lett. **47A**, 66 (1974).
19. M. Ya. Amusia, A. S. Baltenkov, L. V. Chernysheva et al., Phys. Rev. A **63**, 052506 (2001).
20. J. W. Cooper, Phys. Rev. A **42**, 6942 (1990); **45**, 3362 (1992); **47**, 1841 (1993).
21. A. Bechler and R. H. Pratt, Phys. Rev. A **42**, 6400 (1990).
22. M. Ya. Amusia, *Atomic Photoeffect*, Plenum Press, New York–London (1990).
23. M. Ya. Amusia and L. V. Chernysheva, *Computation of Atomic Processes*, "Adam Hilger" Institute of Physics Publishing, Bristol–Philadelphia (1997).
24. M. Ya. Amusia, A. S. Baltenkov, and B. G. Krakov, Phys. Lett. A **243**, 99 (1998).
25. M. Ya. Amusia, A. S. Baltenkov, V. K. Dolmatov et al., Phys. Rev. A **70**, 023201 (2004).
26. M. Ya. Amusia, in: *VUV and Soft X-ray Photoionization*, ed. by U. Becker and D. A. Shirley, Plenum Press, New York (1996), p. 1.
27. J. Berkowitz, J. Chem. Phys. **111**, 1446 (1999).
28. S. W. J. Scully, E. D. Emmons, M. F. Gharaibeh et. al., Phys. Rev. Lett. **94**, 065503 (2005).